Numerical Modeling of a Pile Group Subjected to Seismic Loading Using the Hypoplasticity Model

Ahmed Salman Jawad
Civil Engineering Department
College of Engineering
University of Baghdad
Baghdad, Iraq
a.jawad1901p@coeng.uobaghdad.edu.iq

Bushra S. Albusoda
Civil Engineering Department
College of Engineering
University of Baghdad
Baghdad, Iraq
dr.bushra_albusoda@coeng.uobaghdad.edu.iq

Received: 21 September 2022 | Revised: 14 October 2022 | Accepted: 15 October 2022

Abstract-Various simple and complicated models have been utilized to simulate the stress-strain behavior of the soil. These models are used in Finite Element Modeling (FEM) for geotechnical engineering applications and analysis of dynamic soil-structure interaction problems. These models either can't adequately describe some features, such as the strain-softening of dense sand, or they require several parameters that are difficult to gather by conventional laboratory testing. Furthermore, soils are not completely linearly elastic and perfectly plastic for the whole range of loads. Soil behavior is quite difficult to comprehend and exhibits a variety of behaviors under various circumstances. As a result, a more realistic constitutive model is needed, one that can represent the key aspects of soil behavior using simple parameters. In this regard, the powerful hypoplasticity model is suggested in this paper. It is classified as a non-linear model in which the stress increment is stated in a tonsorial form as a function of strain increment, actual stress, and void ratio. Eight material characteristics are needed for the hypoplastic model. The hypoplastic model has a unique way to keep the state variables and material parameters separated. Because of this property, the model can implement the behavior of soil under a variety of stresses and densities while using the same set of material properties.

Keywords-constitutive modeling; hypoplasticity; pile; PLAXIS 3D; seismic loading

I. INTRODUCTION

Piles are an extensively utilized deep foundation type and are usually adopted in heavy building constructions on weak soils due to their large bearing capacity, low distortion, and high reliability [1-3]. The behavior of piles under seismic stress is a complicated soil–structure interaction phenomenon that can compromise the stability of pile-supported structures to risk. In seismically active places and during earthquakes, movements go from stiffer to softer near-surface layers, they tend to increase and pass to the superstructure via the piles. As a result, structural vibrations develop in the superstructure, imposing inertial pressure on the pile cap and pilings and if the inertial load is big enough, the piles experience substantial lateral displacement and bending moment and consequently piling foundations may be severely damaged. So, in seismically active locations, proper geotechnical and structural design techniques for pile foundations are essential. The earthquake usually creates an additional loading situation on the pile that needs special attention [4-6].

Numerical modeling by FEM of experimental efforts is comparatively advantageous, and is one of the preferred approaches widely utilized for the modeling of the behavior of piled foundations under earthquakes [7-8]. It has been noted that FEM typically produces reliable findings that meet with the experiments. In [9], a comparison of the shaking table test and numerical model was performed to simulate the piled raft foundation in a dry bed of deposited sand. The system was subjected to a strong ground motion while the simulated model was linear visco-elastic. The authors showed that the experimental and numerical results match. The effect of pile soil interaction on resistance and stiffness of pile with sandy soil was investigated under centrifuge loading in [10]. The study adopted finite element analysis to simulate the models. The test results were compared with the analytical solution in terms of bearing capacity. It was reported that the interaction effect between raft and piles reduces the stiffness of the pile group. At the same time, the increment in vertical and horizontal stresses due to the presence of the raft on subsoil causes an enhanced pile response. A three dimensional finite element numerical analysis was performed using PLAXIS 3D to investigate the behavior of pile-caps under seismic and time history loading as settlement and load shearing between the piles and foundation in [11] and the results were verified with experimental work. The maximum amplitude of displacement was decreased by burying the pile cap deeper into the ground and increasing its thickness. Furthermore, reducing the foundation's dynamic reaction was also accomplished by increasing the separation between the foundation and the relative density of the sand. 3D numerical finite element simulation with ABAQUS was conducted to predicate single-pile and pile-system behavior in soft, saturated kaolin clay during various earthquakes in [12]. The results were verified with the centrifuge results from [13]. The linear elastic model was utilized for the piles and the nonlinear kinematic hardening model with Von Misses failure criterion for the clay. The

Corresponding author: Ahmed Salman Jawad

simulation results were in good agreement with the observed acceleration and bending moment. Also, the distance between piles in a pile group had a significant influence on the amount of interaction, acceleration response, forces, and bending moments. In [14], numerical analysis was conducted to predicate the response of pile and soil-pile-stricture interaction with ground improvement (cement mixing method) using ABAQUS. A single pile model with superstructure was used to examine soil-pile-structure interaction behavior with head masses of 25, 100, and 160lbs. During the Loma Prieta earthquake, the piles had a maximum horizontal acceleration of 0.16g. The simulation results agreed well with the acceleration time history at the pile head of 160lbs mass.

The hypoplasticity model was first proposed in [15] and has been in development since then. Due to the complicated calculations of such a model, FEM is used via commercially available FEM software, e.g. Plaxis, FEAT, and ABAQUS. Some of these do not have hypoplasticity as a built-in model. This problem is solved by using the subroutine UMAT with PLAXIS 3D to provide the necessary tensor entries. PLAXIS 3D was used in this research due to the high capability of the software to deal with the elastic-plastic, non-linear, and contact problems [16]. This paper aims to use the hypoplasticity model in soil structure interaction problems.

II. EXPERIMENTAL WORK

The hypoplastic model needs eight material parameters (φ_c, e_{c0}, e_{i0}, e_{d0}, n, hs, α, β). In order to obtain these model parameters, a series of physical-mechanical tests was performed on sand from Baghdad city, which was utilized in this study. Its physical properties are summarized in Table I.

TABLE I. PHYSICAL PROPERTIES OF SAND SAMPLE

Test name	Soil property	Value
Specific Gravity Gs	Specific gravity	2.64
Standard Compaction Test	Maximum dry unit weight γ_{max} (kN/m^3)	16.55
	Minimum dry unit weight γ_{min} (kN/m^3)	13.85
	Maximum void ratio, e_{max}	0.87
	Minimum void ratio, e_{min}	0.56
Grain size analysis	Coefficient of uniformity, C_u	3.33
	Coefficient of curvature, C_c	0.83
	Unified Soil Classification System (USCS)	SP

III. HYPOPLASTICITY MODEL INPUT PARAMETERS

A. Void Ratio (e)

The void ratio is an essential factor in the calculation of the parameter model. Three parameters are associated with the void ratio. The relationships $e_{min} \approx e_{d0}$, $e_{max} \approx e_{c0}$, and $\frac{e_{i0}}{e_{max}} = 1.2$ [17] can be employed.

B. Critical Angle of Friction (φ_c)

The critical angle of friction can be determined for loosely dry sand (particle size greater than 0.1mm) by the conduction angle of repose while for finer soil (particle size less than 0.1mm), the critical angle of friction can be determined by classical mechanical soil tests [18].

C. Stiffness Parameters (n and h_S)

The soil stiffness in the hypoplasticity model relies on the h_s and n parameters and is determined by the confined compression test on loose dry sandy soil [19]. C_c (the compression curve slope) describes the slope of the curve derived from the confined compression test and displayed in the ln σ vs. e plane:

$$c_c = \frac{\Delta e}{\Delta \ln \sigma} \quad (1)$$

The k_o value along the normal consolidation line remains constant throughout the proportional loading, and k_o is determined using Jacky's formula [19]:

$$k_0 = 1 - \sin \varphi_c \quad (2)$$

Then, the value of k_o is used to find the p by:

$$\ln \sigma = \ln\left(\frac{3}{1+2k_0} p\right) = \ln\left(\frac{3}{1+2k_0}\right) + \ln p \quad (3)$$

Equation (4) used to get the value of n from the two values of C_c shown in Figure 1 [20] for two distinct values of (p_s):

$$n = \frac{\ln\left(\frac{e_1 c_{c2}}{e_2 c_{c1}}\right)}{\ln\left(\frac{p_2}{p_1}\right)} \quad (4)$$

By applying (5), the h_s can be calculated from the range of p_1 and p_2:

$$h_s = 3p\left(\frac{ne}{c_c}\right)^{\frac{1}{n}} \quad (5)$$

The compression curve is influenced by the stiffness parameters (h_s and n), where the former governs the curve's overall slope and the latter its curvature [19].

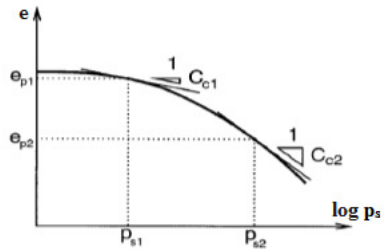

Fig. 1. Confined compression test results are used to determine the h_s and n parameters [20].

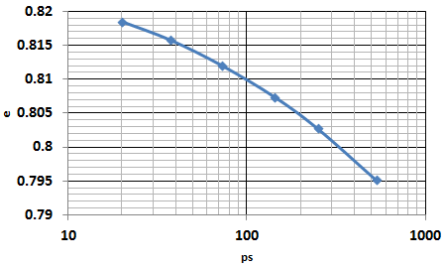

Fig. 2. Confined compression test on loosely dry sample.

Three confined compression tests were conducted on loosely dry sand soil with an initial void ratio e of 0.82 and 800kPa maximal normal stress was applied to them. As part of the sample preparation procedure, the sand was poured down a zero-height funnel to create the loosest condition [20]. The results from the confined compression test performed on loosely sand sample are shown in Figure 2.

D. α and β Parameters

The α parameter is obtained from the triaxial Consolidated Drained (CD) Test carried out on the dense sandy sample with initial void ratio e = 0.62, corresponding with Relative Density Dr = 80.6% and different confining pressures of 50, 100, and 200kPa as shown in Figures 3 and 4. From these tests, the α parameter was found to be equal 0.136 while the hypoplasticity model β can be set to 1 for natural [20]. The final values of the hypoplasticity model are summarized in Table II.

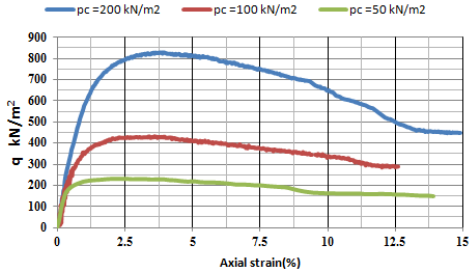

Fig. 3. Deviatoric stress vs. axial strain of the triaxial CD test.

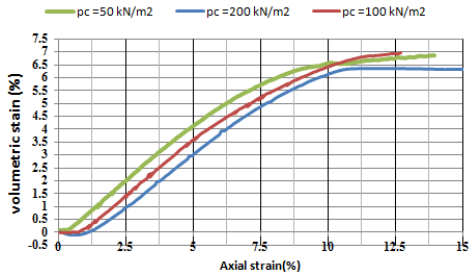

Fig. 4. Volumetric strain vs. axial strain of the triaxial CD test.

TABLE II. HYPOPLASTICITY MODEL PARAMETER VALUES USED IN THIS RESEARCH

Parameter	Value
Critical friction angle φ_c	30
Minimum, maximum, and critical void ratio at zero pressure ed_0, e_{c0}, e_{i0}	0.56, 0.87, 1.044
Granular hardness h_s (MPa)	4000
Exponent relating to sensitivity of granular skeleton to changes of pressure n	0.419
Exponent describing the transition between peak and critical stress α	0.136
Exponent representing the change of stiffness at current density β	1

IV. VALIDATION PROBLEM

In order to validate the program's capabilities in modeling the hypoplasticity problem, the findings from experimental, numerical (Open Sees, SANI SAND model), and PLAXIS 3D hypoplasticity analysis were compared. The problem involved a comparison between the results obtained from the experimental and numerical research performed by [22-24] and the results obtained from PLAXIS 3D. The problem includes conducting a number of centrifugal tests to assess the interaction between the soil and the structure of layered liquefiable soil deposits and the seismic site response. The total depth of the soil profile was 18m, consisting of a 3 layered soil of 2m coarse sand crust with a relative density Dr = 90%, a 6m loose sand layer with Dr = 40%, and a 10m dense sand layer with Dr = 90% at the bottom.

A. Finite Element Modeling

The geometry of the problem was modeled using finite elements under PLAXIS 3D. It is similar to that adopted in the experimental work as shown in Figure 5. A scaled version of the recorded Kobe earthquake was applied at the base of the model, which was referred to as the Kobe-L motion.

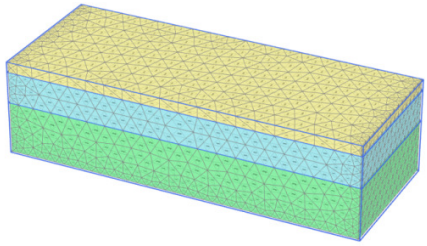

Fig. 5. The finite element model adopted in PLAXIS 3D.

B. Soil Modeling

The material behavior of sand in this study was modeled by the hypoplasticity model and the parameters of its implementation were determined by [21] as shown in Table III.

TABLE III. PARAMETERS OF THE HYPOPLASTICITY MODEL

Parameter	Value
φ_c	30
ed_0, e_{c0}, e_{i0}	0.53, 0.82, 0.94
h_s (MPa)	2000
n	0.22
α	0.25
β	1

C. Result Comparison

A comparison between the experimental test and PLAXIS 3D results is shown in Figures 6 and 7. It can be seen that the results of maximum settlement are approximately compatible with the results of finite element analysis with slightly difference at 8m depth. The vertical settlement, however, is evolving considerably more quickly according to the model than what was actually seen during the experiment, even though they are still in good agreement. The results of excess pore water pressure show a good agreement between the experimental results and numerical analysis. Finally, it can be concluded that the proposed (hypoplasticity) model and PLAXIS 3D software can manipulate the dynamic analysis with good accuracy and are considered an appropriate tool for studies of the soil pile interaction effects.

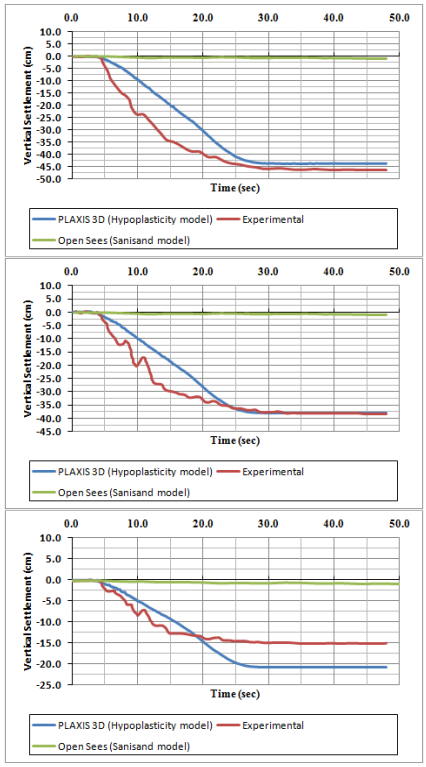

Fig. 6. Experimentally measured, numerically computed (open sees) settlement versus time after [23] and PLAXIS 3D results at depth (a) 0m, (b) 2m, and (c)=8m.

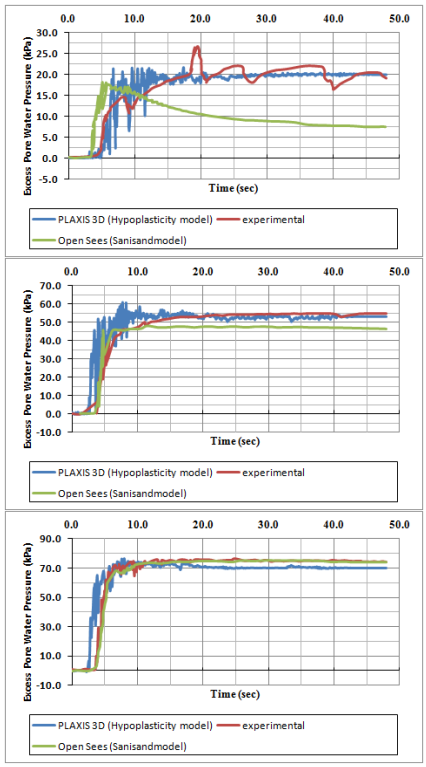

Fig. 7. Experimentally measured, numerically computed (open sees) excess pore water pressure versus time after [23] and PLAXIS 3D results at depth (a) 0m, (b) 2m, and (c) 8m.

V. PARAMETRIC STUDY

In this research, the behavior of the piled-raft system is analyzed using PLAXIS 3D under varying seismic loading. The analysis is focused on the pile response under seismic loading. Three different elements are included in the model: volume element for the soil, plate element for the raft, and building and embedded beams for the piles as shown in Figure 8.

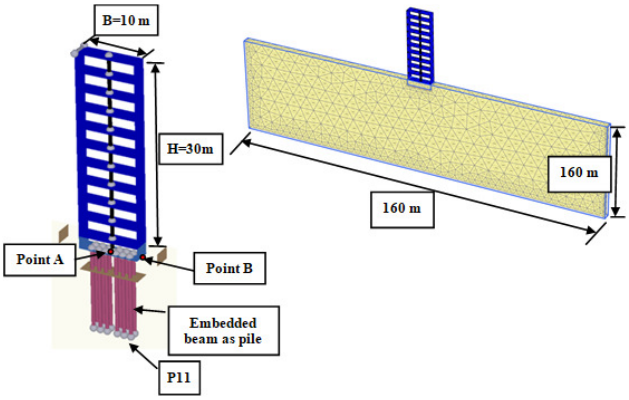

Fig. 8. 3D finite element model.

A. Material Properties

The properties of the sandy soil are shown in Table II. The piles have been modeled as embedded circular massive beams with 0.3m diameter.

B. Earthquake Data

Earthquake records data were utilized to study the effects of acceleration characteristics within soil and pile. Two different real acceleration records, namely Upland and Kobe earthquakes were used (Table IV and Figure 9).

TABLE IV. INFORMATION REGARDING THE EARTHQUAKE DATA [25]

Earthquake	Upland	Kobe
Region	Los Angeles area, Southern California, USA	Japan
Magnitude (MW)	5.7	6.9
Date (UTC)	1990-02-28 23:43:36	1995-01-16 20:24:52
Shaking duration (s)	20	48
Acceleration direction	N-W	N-S
Maximum acceleration (g)	0.24	0.82
Epicenter depth (km)	10	7.9
Station code	CLMCV	KIMA
Station distance to the epicenter (km)	120.3	1.0
Modified Mercalli intensity (MMI)	VII –Very Strong	VII –Very Strong
Reference	[25]	

(a)

(b)

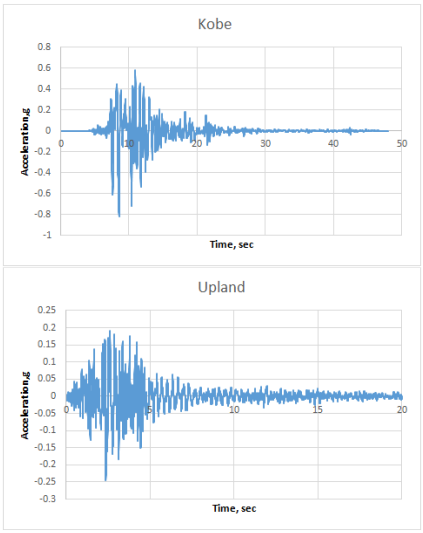

Fig. 9. Earthquake record.

C. Results and Discussion

1) Effect of Pile Length and Pile Spacing on Vertical Settlement

The effect of pile spacing (2D, 3D, and 4D) on the response of the piled raft subject to earthquake excitation is studied in this section. Figures 10-14 show the time history of the soil settlement measured in the middle of raft (A) and at the edge of raft point (B) for both earthquake motions.

(a)

(b)

(c)

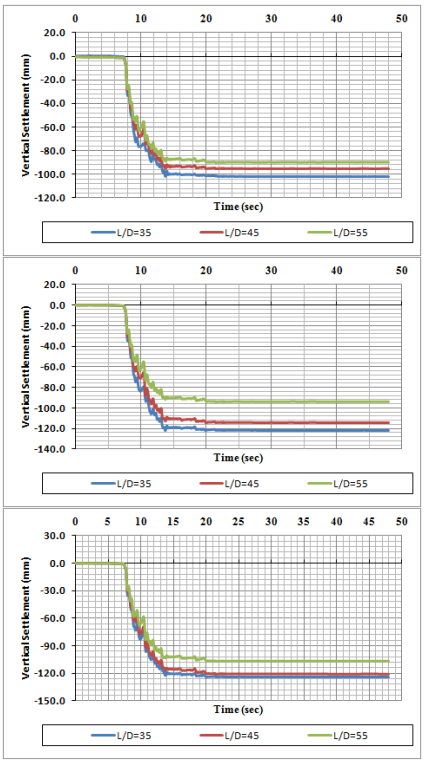

Fig. 10. Variation of the vertical settlement with time at point (A) during the Kobe earthquake at S/D = (a) 2, (b) 3, (c) 4.

(a)

(b)

(c)

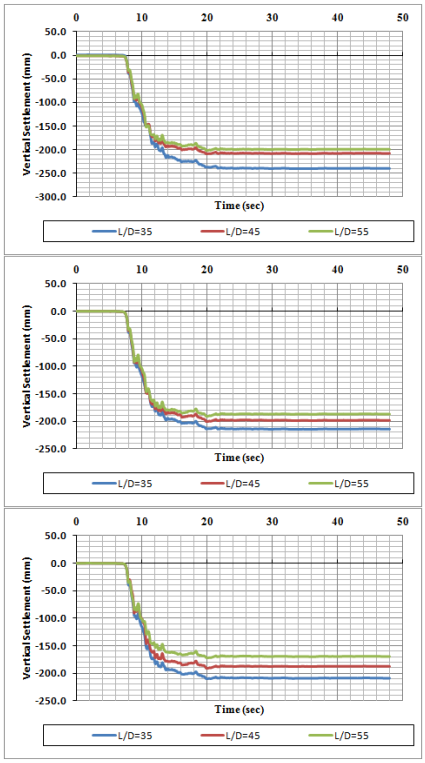

Fig. 11. Variation of the vertical settlement with time at point (B) during the Kobe earthquake at S/D = (a) 2, (b) 3, (c) 4.

(a)

(b)

(c)

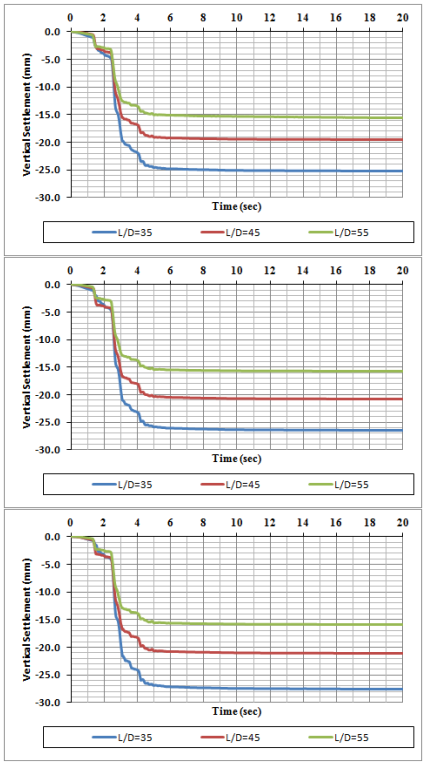

Fig. 12. Variation of the vertical settlement with time at point (A) during the Upland earthquake at S/D = (a) 2, (b) 3, (c) 4.

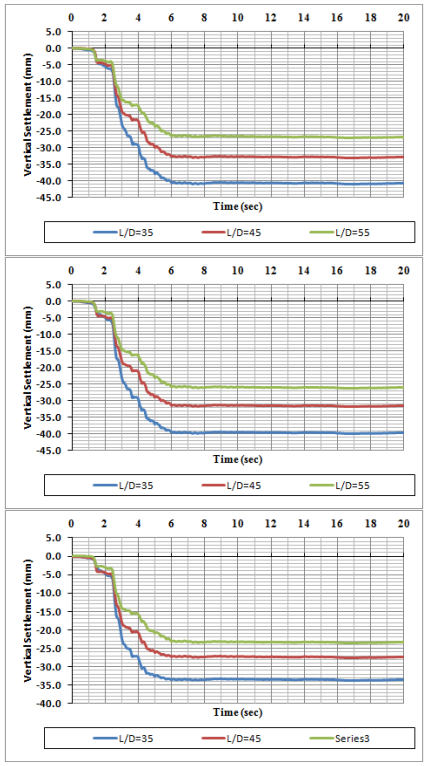

Fig. 13. Variation of the vertical settlement with time at point (B) during the Upland earthquake at S/D = (a) 2, (b) 3, (c) 4.

It can be concluded that increasing the spacing among piles to 3D and 4D from the basic 2D spacing increases the total settlement. This behavior could be attributed to the decrease in spacing between piles that applied additional lateral forces between soil particles by holding them together and providing confining media. This action resists the external forces thus decreasing total settlement. This force affects the piles as well as soil particles leading more friction forces at the pile surfaces as the friction is a function of normal forces and the friction coefficient, so increasing the skin friction leads to more resistance in total settlement as a result. The decrease in spacing between piles means that the piles are concentrated at the middle of the raft which resists the dishing effect occurring in the sand. This action leads to a decrease in probable total settlement as the maximum settlement occurs in the middle of the raft in the case of sand due to the dishing phenomenon. Finally, it can be concluded that total settlement increases as the pile spacing increases. Similar observation was noticed in [26-27]. For increasing pile length, load transfer is affected by the pile length. This factor is considered by selection of 3 different piles lengths (L/D) equal to 35, 45, and 55. Based on numerical analysis, it is found that the increase of pile length decreases the total settlement of piled foundation as shown in Figures 10-14. This behavior can be attributed to the increase of the pile length which absorbs more power applied from earthquakes and dissipates the applied forces since the settlement is a function of the applied load [26-32].

Earthquake excitation has a major influence on the piled raft behavior. Piled raft foundation placed on loose dry soil and subjected by Kobe and Upland earthquake motions was modeled numerically to investigate the effect of the excitation on the total settlement (Figures 10-14). From these Figures, it can be concluded that the total settlement of pile raft increases as the earthquake excitation increases. Higher excitation leads to higher dynamic loading, which results in higher settlement, as the settlement is a function of loading.

2) Effect of Pile Length and Pile Spacing on Maximum Pile Bending Moment

Pile foundations can be divided into two categories based on the ratio of the effective unsupported length (L) to the average pile diameter (D), where L/D > 30 denotes a long pile and L/D ≤ 20 denotes a short pile [28]. The effect of length to pile diameter L/D (35, 45, and 55) and pile spacing S/D (2, 3, and 4) on the response of piled raft subjected to two earthquake excitations is illustrated in Figures 15-17. The following points can be noted: The maximum bending moment occurred at the connection between the piles and the raft and the zero moment is located near the tip of the pile. Also, it can be concluded that increasing the spacing among piles to 3D and 4D 2D increases the bending moment along the pile shaft. This behavior can be explained by the fact that higher excitation leads to higher dynamic loading which results in higher bending moment.

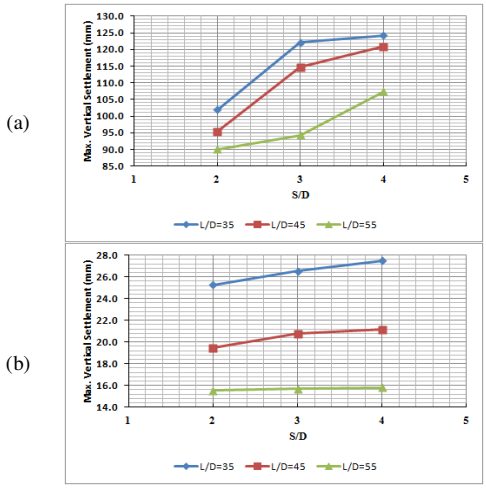

Fig. 14. Variation of max. vertical settlement with S/D at point (A) for (a) Kobe and (b) Upland earthquake.

The effectiveness of the constitutive models employed in the modeling of the soil-pile interaction under the influence of earthquake motion is a key factor in the precise simulation of the numerical analysis in geotechnical engineering. There are limited numerical investigations of the behavior of soil-pile interaction using various constitutive models. Each of these models has its own unique features and advantages, most fall short of providing an adequate description of this behavior. Due to this factor, the analysis of soil-pile-structure systems subjected to seismic stress using an efficient model (the hypoplasticity model) is the goal of this study. The hypoplasticity constitutive model is implemented using the UMAT subroutine, which is then incorporated as a dynamic linked library (DLL) in the PLAXIS 3D finite element program.

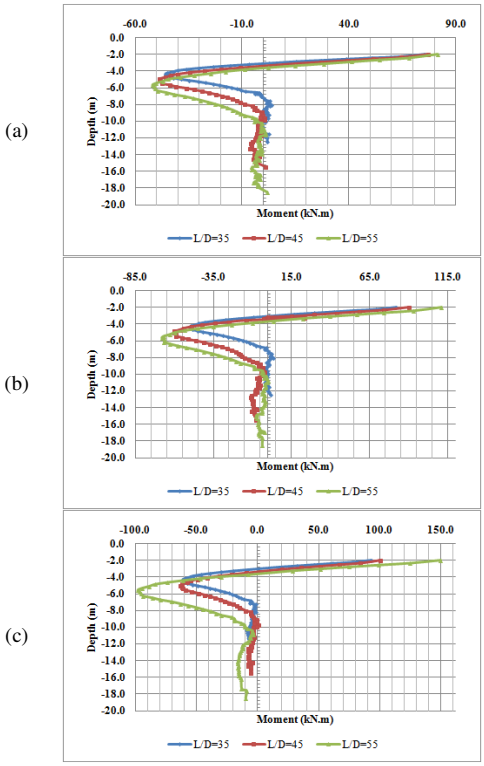

Fig. 15. Variation of bending moment along pile (P11) at peak ground acceleration during the Kobe earthquake at S/D = (a) 2, (b) 3, (c) 4.

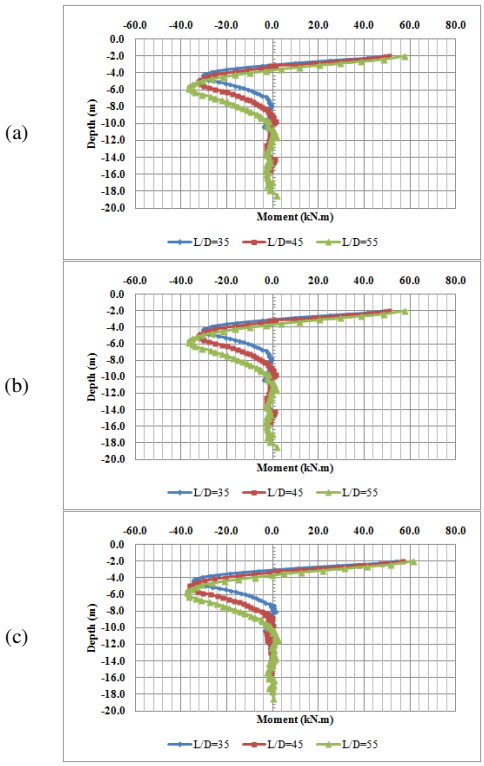

Fig. 16. Variation of bending moment along pile (P11) at peak ground acceleration during the Upland earthquake at S/D = (a) 2, (b) 3, (c) 4.

This model predicts with accuracy the soil response to various soil densities, stress levels, and loading conditions. It also requires several parameters that are easy to gather by conventional laboratory testing. The model's ability in modeling soil-pile interaction was validated with results from experimental tests and also with findings from numerical results conducted using the SANISAND constitutive model. A numerical model of a 10-story building supported by pile systems (soil-pile structure) was examined in order to look into the effects of various interactional parameters. To examine the impact of the excitation frequency, two seismic motions were used. Additionally, the effects of various pile lengths and spacings were examined.

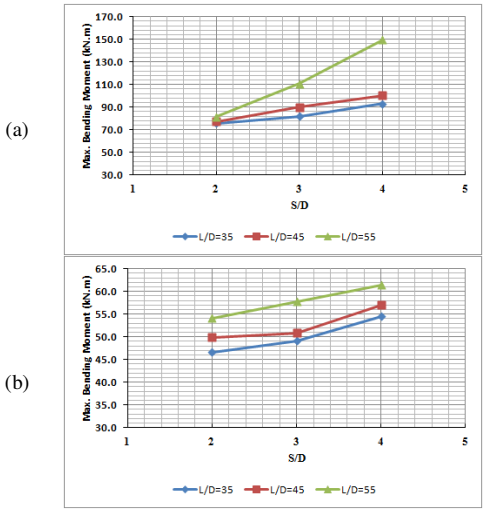

Fig. 17. Variation of max. bending moment with S/D at pile (P11) at peak ground acceleration for (a) Kobe and (b) Upland earthquake.

VI. CONCLUSION

The hypoplasticity constitutive model and the finite element method were used in this study to investigate the dynamic soil pile interaction. The soil parameters for this model were obtained by laboratory tests and were calibrated according to known relationships. The main conclusions from this study are:

- The hypoplasticity constitutive model is quite satisfactory in representing the behavior of the response of the pile foundation under earthquake excitation.
- Increasing in the length of piles decreases the settlement of the piled raft system.
- Increasing the spacing between piles increases the settlement of the piled raft system.
- Increasing the length and pile spacing increases the bending moment.

REFERENCES

[1] R. A. Rajapakse, *Geotechnical Engineering Calculations and Rules of Thumb*, 1st ed. Oxford, UK: Butterworth-Heinemann, 2008.

[2] R. Mackevicius, "Possibility for Stabilization of Grounds and Foundations of Two Valuable Ancient Cathedrals on Weak Soils in

Baltic Sea Region with Grouting," *Procedia Engineering*, vol. 57, pp. 730–738, Jan. 2013, https://doi.org/10.1016/j.proeng.2013.04.092.

[3] M. Tatyana, N. Alexander, and C. Anastasia, "Reinforced Sandy Piles for Low-rise Buildings," *Procedia Engineering*, vol. 117, pp. 239–245, Jan. 2015, https://doi.org/10.1016/j.proeng.2015.08.156.

[4] M. T. A. Chaudhary, M. Abe, and Y. Fujino, "Identification of soil–structure interaction effect in base-isolated bridges from earthquake records," *Soil Dynamics and Earthquake Engineering*, vol. 21, no. 8, pp. 713–725, Dec. 2001, https://doi.org/10.1016/S0267-7261(01)00042-2.

[5] B. Manna and D. K. Baidya, "Dynamic nonlinear response of pile foundations under vertical vibration—Theory versus experiment," *Soil Dynamics and Earthquake Engineering*, vol. 30, no. 6, pp. 456–469, Jun. 2010, https://doi.org/10.1016/j.soildyn.2010.01.002.

[6] M. T. A. Chaudhary, "FEM modelling of a large piled raft for settlement control in weak rock," *Engineering Structures*, vol. 29, no. 11, pp. 2901–2907, Nov. 2007, https://doi.org/10.1016/j.engstruct.2007.02.001.

[7] G. W. Blaney, "Dynamic Stiffness of Piles," in *International Conference on Numerical Methods in Geotechnical Engineering*, Blacksburg, VA, USA, 1976, pp. 1001–1012.

[8] S. Prakash, S. Kumar, and K. Sreerama, "Pile-soil-pile interaction effects under earthquake loadings," in *Eleventh World Conference on Earthquake Engineering*, Acapulco, Mexico, Jun. 1996.

[9] D. Pitilakis, M. Dietz, D. M. Wood, D. Clouteau, and A. Modaressi, "Numerical simulation of dynamic soil–structure interaction in shaking table testing," *Soil Dynamics and Earthquake Engineering*, vol. 28, no. 6, pp. 453–467, Jun. 2008, https://doi.org/10.1016/j.soildyn.2007.07.011.

[10] D. Giretti, "Modeling of piled raft foundations in sand," Ph.D. dissertation, University of Ferrara, Ferrara, Italy, 2010.

[11] I. G. Abdulwahhab, "Experimental and Numerical Approach for the Behavior of Machinery Piled Raft Foundation Embedded within Cohesionless Soils," M.S. thesis, University of Technology, Baghdad, Iraq, 2017.

[12] M. S. Asheghabadi and X. Cheng, "Investigation of Seismic Behavior of Clay-Pile Using Nonlinear Kinematic Hardening Model," *Advances in Civil Engineering*, vol. 2020, Jul. 2020, Art. no. e9617287, https://doi.org/10.1155/2020/9617287.

[13] L. Zhang, S. H. Goh, and H. Liu, "Seismic response of pile-raft-clay system subjected to a long-duration earthquake: centrifuge test and finite element analysis," *Soil Dynamics and Earthquake Engineering*, vol. 92, pp. 488–502, Jan. 2017, https://doi.org/10.1016/j.soildyn.2016.10.018.

[14] T. Thanapon and A. Goran, "Three-Dimensional Analysis of Soil-Pile-Structure Interaction Problem on High Rise Building on Improved Soft Soil," *International Journal of Geomate*, vol. 21, no. 88, pp. 54–60, Dec. 2021, https://doi.org/10.21660/2021.88.gxi293.

[15] D. Kolymbas, "A generalized hypoelastic constitutive law," in *Proceedings of the 11th international conference on soil mechanics and foundation engineering*, San Francisco, CA, USA, 1988.

[16] B. Hua, C. Hao, J. Zhao, C. Wang, X. Zhang, and G. Wang, "Nonlinear FEM analysis of bearing capacity and sedimentation of single pile in multi-layered soils," in *Proceedings of the International Conference on Computing in Civil and Building Engineering*, Shanghai, China, 2010.

[17] K. E. Anaraki, "Hypoplasticity Investigated: Parameter Determination and Numerical Simulation," M.S. thesis, Delft University of Technology, Delft, Netherlands, 2008.

[18] T. Kadlicek, T. Janda, and M. Sejnoha, "Calibration of Hypoplastic Models for Soils," *Applied Mechanics and Materials*, vol. 821, pp. 503–511, 2016, https://doi.org/10.4028/www.scientific.net/AMM.821.503.

[19] R. Suchomel and D. Masin, "Calibration of an advanced soil constitutive model for use in probabilistic numerical analysis," in *1st International Symposium on Computational Geomechanics*, Juan-les-Pins, France, Dec. 2009, pp. 265–274.

[20] D. Masin, "Hypoplasticity for practical applications part 4: determination of material parameters," Ph.D. dissertation, University of Prague, Prague, Czech Republic, 2015.

[21] I. Herle and G. Gudehus, "Determination of parameters of a hypoplastic constitutive model from properties of grain assemblies," *Mechanics of Cohesive-frictional Materials*, vol. 4, no. 5, pp. 461–486, 1999, https://doi.org/10.1002/(SICI)1099-1484(199909)4:5<461::AID-CFM71>3.0.CO;2-P.

[22] J. Olarte, B. Paramasivam, S. Dashti, A. Liel, and J. Zannin, "Centrifuge modeling of mitigation-soil-foundation-structure interaction on liquefiable ground," *Soil Dynamics and Earthquake Engineering*, vol. 97, pp. 304–323, Jun. 2017, https://doi.org/10.1016/j.soildyn.2017.03.014.

[23] J. Ramirez *et al.*, "Site Response in a Layered Liquefiable Deposit: Evaluation of Different Numerical Tools and Methodologies with Centrifuge Experimental Results," *Journal of Geotechnical and Geoenvironmental Engineering*, vol. 144, no. 10, Oct. 2018, Art. no. 04018073, https://doi.org/10.1061/(ASCE)GT.1943-5606.0001947.

[24] S. S. Nagula, Y.-W. Hwang, S. Dashti, and J. Grabe, "Seismic site response of layered saturated sand: comparison of finite element simulations with centrifuge test results," *International Journal of Geo-Engineering*, vol. 12, no. 1, Sep. 2021, Art. no. 26, https://doi.org/10.1186/s40703-021-00155-2.

[25] "COSMOS," *COSMOS*. http://strongmnotion.org/index.html.

[26] S. Azhar, A. Patidar, and S. Jaurker, "Parametric Study of Piled Raft Foundation for High Rise Buildings," *International Journal of Engineering Research & Technology*, vol. 9, no. 12, pp. 548–555, 2020.

[27] A. El-Attar, "Dynamic analysis of combined piled raft system (CPRS)," *Ain Shams Engineering Journal*, vol. 12, no. 3, pp. 2533–2547, Sep. 2021, https://doi.org/10.1016/j.asej.2020.12.014.

[28] B. S. Albusoda and O. Y. Almashhadany, "Effect of Allowable Vertical Load and Length/Diameter Ratio (L/D) on Behavior of Pile Group Subjected to Torsion," *Journal of Engineering*, vol. 20, no. 12, pp. 13–31, 2014.

[29] L. Salem, "Effect Of Pile Spacing On The Behavior Of Piled Raft Foundation Under Free Vibration And Earthquake," *Australian Journal of Basic and Applied Sciences*, vol. 10, no. 12, pp. 240–247, Jan. 2016.

[30] M. O. Karkush, "Impacts of Soil Contamination on the Response of Piles Foundation under a Combination of Loading," *Engineering, Technology & Applied Science Research*, vol. 6, no. 1, pp. 917–922, Feb. 2016, https://doi.org/10.48084/etasr.616.

[31] J. A. Alomari, "The Effect of Mass, Depth, and Properties of the Soil Below the Raft Foundation on the Seismic Performance of R.C. Plane Frames," *Engineering, Technology & Applied Science Research*, vol. 9, no. 5, pp. 4685–4688, Oct. 2019, https://doi.org/10.48084/etasr.2943.

[32] T. Nagao and D. Shibata, "Experimental Study of the Lateral Spreading Pressure Acting on a Pile Foundation During Earthquakes," *Engineering, Technology & Applied Science Research*, vol. 9, no. 6, pp. 5021–5028, Dec. 2019, https://doi.org/10.48084/etasr.3217.